analytical chemistry

pubs.acs.org/ac
Article

Harmonization of FT-ICR-MS Instruments for Interoperable Multi-Laboratory Comprehensive Compositional Profiling

Stefan A. Pieczonka, Mary J. Thomas, Philippe Schmitt-Kopplin,* and James W. Marshall*

Cite This: *Anal. Chem.* 2025, 97, 8491−8498
Read Online

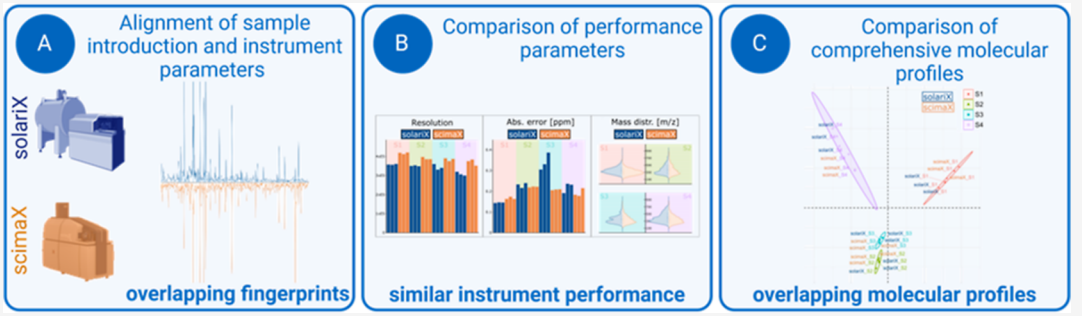

ABSTRACT: Given the long hardware lifespan, fixed installation, and comparatively high investment required to procure them, Fourier transform ion cyclotron resonance mass spectrometry (FT-ICR MS) instruments tend to have a long operational life. The field is constantly evolving with rapidly advancing instrumental developments, and FT-ICR research groups work with a range of instrument designs from different generations. Consequently, compositional spectra comparability between instruments is a critical concern in FT-ICR-MS, particularly due to the variability introduced by commonly used direct infusion methods. This study demonstrates interlaboratory comparability of FT-ICR-MS molecular profiles using a 12 T solariX with an Infinity Cell and a 7 T scimaX with a ParaCell, with closely matched sample introduction and ion guide systems. Using analytically challenging pet food samples, we achieved similar instrument performance metrics, including resolving power, mass error, feature count, signal-to-noise ratios, and m/z distribution. The improved field homogeneity and sensitivity of the ParaCell reduced ICR cell space-charge interferences, making specialized calibration methods beyond linear calibration obsolete. We observed up to 78% overlap in annotated signals of the spectra increasing to 95%, when higher-intensity features are considered. Relative abundances showed great similarity, despite sample-dependent fluctuations (median coefficient of variation 23.4% to 49.2% and 15.5% to 29.5%, respectively). Unsupervised multivariate analysis (PCA) revealed consistent sample profiles with no systematic bias. Our study demonstrates that with careful instrument adjustment, molecular profile comparability can be achieved, ensuring the continued relevance of extensive databases and large chemical data sets acquired in long-term and collaborative projects measured on different instrumentation.

INTRODUCTION

In the past decade, Fourier transform ion cyclotron resonance mass spectrometry (FT-ICR-MS) instrumentation has significantly advanced,[1] particularly with enhancements to ion optics and the ICR cell. A notable development includes the commercialization and routine use of the dynamically harmonized cell or ParaCell.[2,3] The ParaCell technology and 2 ω detection have significantly enhanced the ability of FT-ICR-MS instruments to investigate isotopic fine structures and improved signal-to-noise ratios and acquisition scan speeds, markedly improving methods and applications across a range of fields, including MALDI imaging of tissues,[4] analysis of peptide fine structures,[5] crude oil,[6] and GC-APCI characterization of contaminated soil and biofuels.[7] The reduction in measurement time facilitated by the advances in FT-MS detection technology enables enhanced compositional coverage through spectral stitching or continuous accumulation of selected ions (CASI) measurements to be achieved more rapidly.[8]

While the ParaCell technology is now commercially available, the older generation of instruments featuring the Infinity Cell is approaching the expected end of its production and service lifecycle. In the context of relatively high-investment, stationary, and durable mass spectrometers such as FT-ICR instruments, this ongoing evolution raises the question of whether advancements will render data from previous generations of FT-MS instrumentation obsolete

Received: January 21, 2025
Revised: March 12, 2025
Accepted: March 12, 2025
Published: April 10, 2025

https://doi.org/10.1021/acs.analchem.5c00488
Anal. Chem. 2025, 97, 8491−8498

beyond isolated studies, potentially diminishing the value of established databases and community efforts, or if interoperability among compositional profiles can be achieved.

The outstanding resolving power and mass accuracy of FT-ICR-MS enable direct infusion of samples, an injection method inherently challenging to control and direct due to ion suppression and other ionization effects resulting in non-quantitative data.[9−12] Hence, concerns regarding the consistency of compositional data across laboratories are regularly addressed. An advantage, however, of reducing spectra to the m/z dimension in direct-infusion is the focus on the immutable absolute values of the compositional masses for alignment. The stability of the remarkable mass accuracy and resolving power in FT-ICR analytics is preserved even in extended projects or extensive databases, as demonstrated in our 6-year ongoing study involving hundreds of samples.[13] To fully leverage these extensive databases within long-term and interconnected projects, the comparability of compositional spectra across instruments and instrument generations is of critical importance.

Hawkes et al.[14] compared dissolved organic matter (DOM) samples across high-resolution FT-instruments with varying setups in 16 laboratories, identifying approximately 1000 common compositions per sample, with annotated signals ranging from about 1200 to 6000 depending on the sample, ionization mode, and laboratory. They found that the weighted average m/z values and the average number of peaks were most dependent on the laboratory, with unsaturated compounds exhibiting greater variance overall. Zherebker et al.[15] observed a similar trend in an interlaboratory comparison of natural organic matter (NOM) humic substance samples. For biological tissue and fluid samples, which inherently exhibit a higher concentration dynamic range of metabolites and thus potential ionization effects, it was noted that intralaboratory batch corrections may be necessary[16] and not all FT-ICR-MS setups are comparable to the desired extent.[17] Overall, achieving interoperability between instruments still poses a significant challenge, as the operating parameters on one instrument cannot necessarily be seamlessly transferred to another. The sensitivity of the instruments and the interrelated effects of each parameter require careful and individualized sample preparation and tuning. These procedures may vary significantly between instruments, especially when comparing biological materials on different instrument generations, to ensure comparable results.[14,18−20]

In this study, we assess the interlaboratory interoperability of ultrahigh resolution FT-ICR-MS compositional profiles between a solariX setup with the Infinity Cell and its modern counterpart, the scimaX ParaCell. We aim to achieve molecular profile comparability by harmonizing sample introduction, ionization, ion transfer, and detection parameters. When successful, these efforts will maintain the relevance and utility of extensive databases and chemical maps from previous-generation instruments. Comparability will be assessed using pet food samples, which, due to their biological origin, mineral additives, and complex processing reactions, represent inherently complex and challenging matrices with a wide dynamic range and significant potential for adverse ionization interferences.

Methodology. *Pet Food Sample Extraction.* One wet pet food product (sample 1, chicken variety meal) and three dry pet food products (sample 2, cheese variety treat; sample 3 tuna variety meal; sample 4 chicken variety meal) were homogenized and extracted at Waltham Petcare Science Institute (Mars Petcare), with "variety" indicating that the specific ingredient must constitute a minimum of 4% of the product. The pet food was homogenized as 1.25 g aliquots with 5 mL of methanol: water (HPLC for Gradient Analysis, Fisher Scientific) and 2.5 mL of hexane (≈95% *N*-Hexane, for HPLC, Fisher Scientific). The nonsoluble lipid fraction (hexane phase) was separated by centrifugation (10,000 rpm). The methanol−water phase was dried (SpeedVac, Thermo Fisher Scientific, Loughborough, UK). Samples were reconstituted in 500 μL of water, centrifuged, filtered through a SFCA syringe filter (0.2 μm; Thermo Fisher Scientific), sealed, and stored at −80 °C prior to FT-ICR-MS analysis in triplicate.

SolariX FT-ICR-MS Measurements. The Bruker solariX ion cyclotron resonance Fourier transform mass spectrometer (Bruker Daltonics GmbH, Germany) equipped with a 12 T superconducting magnet (Magnex Scientific Inc., GB), an Infinity ICR cell, and an APOLLO II electrospray ionization (ESI) source (BrukerDaltonics GmbH, Germany) was operated at Helmholtz Munich (Analytical BioGeoChemistry), Germany. An aliquot of the sample extracts was shipped to Germany on dry ice, maintaining a temperature of −80 °C. The extracts were diluted 1 to 100 with MeOH and centrifuged (12,000 rpm; 5 min), prior to direct infusion of the supernatant to the FT-ICR-MS instruments using a PAL autosampler system (CTC Analytics, Switzerland) at 2 μL/min utilizing a Zirconium Ultra 410F pump (Prolab Instruments GmbH, Switzerland). High-resolution spectra were obtained in negative ionization mode, accumulating 350 scans with an ion accumulation time of 350 ms, culminating in a total measurement time of 10.4 min.

ScimaX FT-ICR-MS Measurements. The Bruker scimaX ion cyclotron resonance Fourier transform mass spectrometer (Bruker Daltonics GmbH, Bremen, Germany) equipped with a 7 T superconducting magnet, a ParaCell, and an APOLLO II ESI source (BrukerDaltonics GmbH, Germany) was operated at Waltham Petcare Science Institute (Mars Petcare, UK). Given the greater sensitivity of the scimaX instrument, samples were run 4× more diluted, and fewer scans (120) could be acquired, in a shorter total experiment time, to achieve similar signal-to-noise ratios. Due to the difference in hardware, including ion optics, different tuning parameters were required in order to reach a similar mass distribution and spectral profile, for example, low mass cut off and ion accumulation time. Aliquots of the sample extracts were stored at −80 °C and diluted 1 to 400 in MeOH (Optima, Fisher Scientific, UK) and centrifuged prior to infusion of the supernatant to the FT-ICR-MS instruments using a PAL RSI autosampler system (CTC Analytics, Switzerland). High-resolution spectra were obtained in negative ionization mode, accumulating 120 scans with an ion accumulation time of 20 ms and time-of-flight of 0.6 ms, culminating in a total measurement time of 4.4 min for 1 omega broadband measurements. The detailed parameters of both instruments are summarized and compared in Table S1.

Data Processing, Integration, and Statistical Analysis. The raw spectra were postprocessed by Compass DataAnalysis 4.2 (Bruker Daltonics, Bremen, Germany). Accurate linear mass calibration of spectra was performed using an in-house calibration list of 3000 persistent, recurrent compounds present in the FT-ICR-MS spectra of pet food samples. A linear calibration up to m/z 600, with mass error below 0.1 ppm, was achieved for both instruments. Acquired masses were

https://doi.org/10.1021/acs.analchem.5c00488
Anal. Chem. 2025, 97, 8491−8498

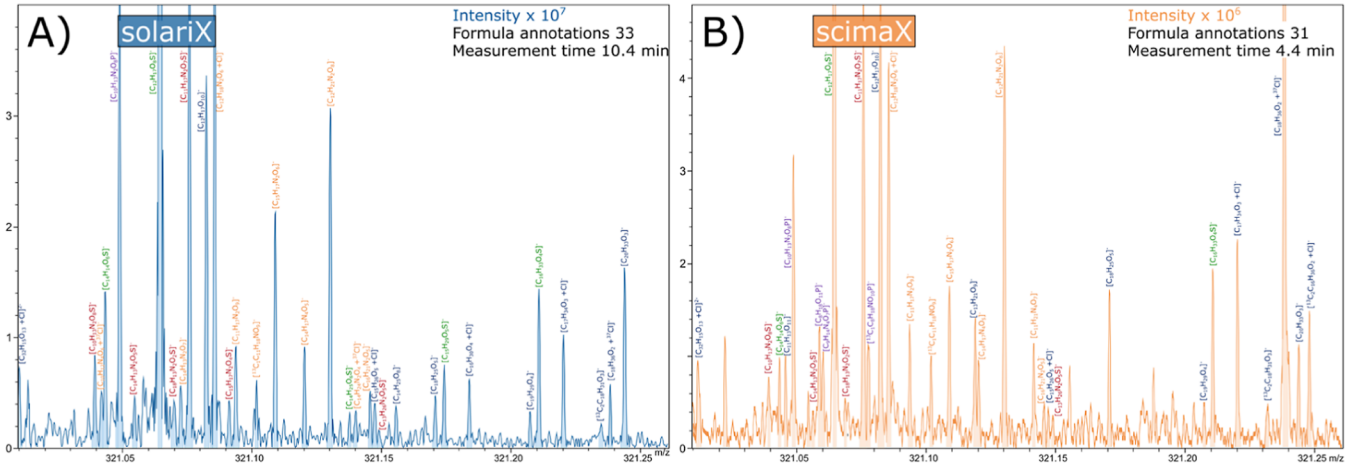

Figure 1. FT-ICR mass spectral excerpts of the nominal mass m/z 321 from sample 1, acquired using the solariX (A) and scimaX (B) instrumental setups. For annotated peaks, the respective molecular formula is given. The different intensity scales indicate a distinct data structure despite a similar fingerprint.

filtered to remove peaks below a signal-to-noise ratio of 4. Different noise levels were addressed by setting distinct absolute intensity thresholds of 2,000,000 (solariX) and 500,000 (scimaX), respectively. The CASI windows were merged for each sample to create a spectrum spanning the entire mass range prior to data filtering. Possible space-charge effects[21] and electric field distortions were recalibrated by mass difference mapping on both individual samples and the merged feature matrix.[22,23] Peak list filtering (FT side loop artifacts and isotopologue peaks) was performed using an in-house R-based (version 4.2.2) software tool on a single spectrum basis following Kanawati et al.[24] Single-charged signals found in at least two out of three replicates were retained. Peak alignment was achieved within a 0.5 ppm threshold. Subsequent peak annotation in the CHNOSPCl compositional space was carried out using a mass difference network.[25]

For data integration, the solariX and scimaX data sets of annotated signals were first processed independently before being merged back into a matrix. Noise imputation (gap-filling) was implemented by replacing null values with random values within the -2σ to -1σ range of the mean of the lowest peak of each sample. Subsequently, the intensity values of each feature across samples of the data set were z-score-normalized and centered. In cases where a feature in one data set shows no intensity value, null values were replaced with normalized noise values from the corresponding data set that exhibits the signal. Within-data set normalized intensities were merged back into a single matrix that included both data sets. To emphasize the necessity for a comprehensive data integration strategy, a contrasting data matrix was created where noise-filling and normalization were executed on the entire matrix instead of individual data sets. PCA statistical analysis was performed using the FactoMineR R package (version 4.2.2). Potential systematic differences between the instrumental setups were assessed using Cohen's d, while differences between samples were evaluated using ANOVA in the RStudio programming environment (version 2023.12.1). Confidence ellipses for the sample classes (samples 1, 2, 3, and 4) were drawn at the 95% level. Annotated peaks characteristic of the molecular profiles of the samples were extracted using a score plot and loading plots overlapping densities.

Instrument Performance Parameters and Data Visualization. The performance of the instrumental setups was compared based on median signal-to-noise ratio, median resolving power, annotated feature count, average mass error to assess systematic errors, absolute average mass error to assess the annotation mass error, and m/z distribution. Median values were chosen to minimize the influence of the outliers. Values were visualized as bar plots, and violin plots using Kernel Density Estimation at a bandwidth of 10 (m/z distribution), respectively. Molecular compositions of specific interest were visualized in van Krevelen diagrams. By plotting H/C versus O/C atomic ratios, it is possible to depict common compositional patterns[26,27] and obtain tentative information on molecule classes.[28,29] An overview of the compositional spaces was plotted as a pie chart.

RESULTS AND DISCUSSION

Evaluation of the Instrumental Setup. In this study, two instrumental setups located in different laboratories, one in Munich, Germany (12 T solariX), and the other in Waltham, United Kingdom (7 T scimaX), collectively representing approximately 20 years of FT-ICR-MS development, were carefully aligned, taking into account community-recommended guidelines,[14,18−20] and subsequently compared. The sample introduction, ion source, and ion transfer parameters were carefully adjusted and tuned to enable operation in a comparable manner, while individual settings were optimized to establish an effective method for both instruments (Table S1). Detection settings in infinity cell (SolariX) and ParaCell (ScimaX) were also aligned. Both instruments were coupled to the same autosampler system for high-throughput operation, ensuring interoperability at scale. Postacquisition data processing strategies were conducted identically, accounting for the lower noise levels of modern cell. This setup allowed us to evaluate whether the compositional data of long-term studies and comprehensive databases generated by previous generation instruments nearing the end of their manufacturer support will become obsolete when replacing the device or if these data can retain their relevance and utility.

While many interlaboratory studies and ring trials focus on applying ultrahigh resolution to environmental NOM or DOM samples,[14,15,18] we have instead targeted complex life sciences

https://doi.org/10.1021/acs.analchem.5c00488
Anal. Chem. 2025, 97, 8491−8498

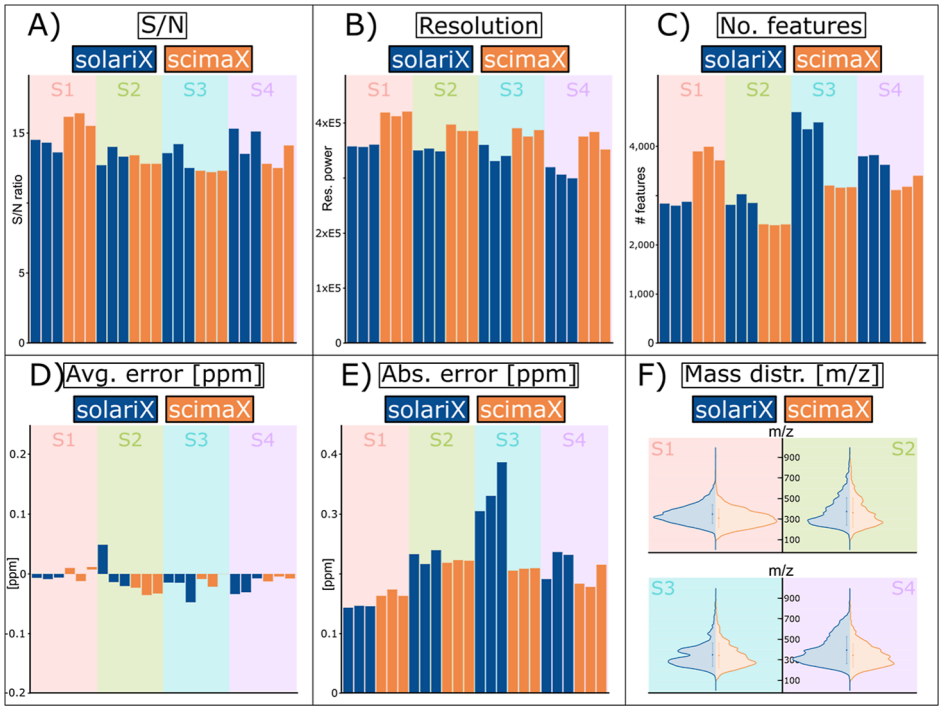

Figure 2. Comparison of the instrument performance of the solariX (blue) and scimaX (orange) systems with respect to median signal-to-noise ratio (A), median resolution value (B), number of features (C), average annotation mass error (D), average absolute annotation mass error (E), and m/z value distribution (F). The attributes are sorted by samples (S1−S4), and each bar corresponds to a replicate measurement.

samples, i.e., pet food. They combine biological origin, mineral additives, complex processing reactions, and a broad dynamic concentration range, making them an arguably challenging matrix. This approach strengthens the plausibility of extending our findings to other biological samples and systems.

Comparison of Instrument Performance. In the four pet food samples measured on both platforms in triplicates, a total of 9948 monoisotopic mass signals were annotated. Of these, 4751 were detected in both setups. On average, 3562 compositions were annotated per measurement and 1892 compositions were present in all samples. To illustrate the data structures, Figure 1 shows the nominal mass m/z = 321 as detected on both instrumental setups. Even within this excerpt of isobaric compounds, the complexity of pet food is evident, making it a suitably challenging matrix to analyze interoperability. Food covers a great deal of variety in the CHNOSPCl chemical space, including representatives of saturated lipids $[C_{20}H_{33}O_3]^-$ to phosphorus-containing compounds $[C_{10}H_{13}N_2O_8P]^-$, sulfur-containing species $[C_{15}H_{29}O_5S]^-$, and unsaturated heterocycles $[C_{14}H_{17}N_4O_5]^-$. Additionally, various adducts $[C_{12}H_{18}N_2O_6{+}Cl]^-$, charge states $[C_{32}H_{15}O_{13}{+}Cl]^{2-}$, and isotopologue compositions $[^{13}C_1C_{11}H_{18}NO_9]^-$, and $[^{13}C_2C_{18}H_{31}O_3]^-$ are observed.

Since the parameters suggested by Hawkes et al.[14] for comparing samples and instrument performances are specifically tailored to DOM or NOM data structures, we focused on the generally relevant instrument performance parameters of annotation mass error, resolution, signal-to-noise ratio, m/z distribution, and number of features (Figure 2). An intensity-based weighting of annotations was not performed, as it would introduce biases due to the large dynamic concentration range of the pet food samples compared with DOM and NOM.

The median signal-to-noise ratios (solariX 13.9 ± 0.9; scimaX 13.6 ± 1.6) and median resolving power (solariX 3.4 × 10^5 ± 0.2; scimaX 3.9 × 10^5 ± 0.2) remained stable at similar levels, independent of the sample or instrument (Figure 2A,B). The underlying number of annotated mass signals naturally exhibited greater variability between the samples and between instrumental setups (solariX 3500 ± 724; scimaX 3228 ± 559). Notably, the inverse trend of more features in sample 1 on the scimaX system and in sample 3 on the solariX system highlights less systematic and more sample-dependent dynamic performance differences between the setups (Figure 2C). The average error in annotation, defined as the average difference between accurately measured mass and the theoretical exact mass of the annotated composition, indicated no systematic errors in formula assignment in either system (solariX −0.02 ± 0.04 ppm; scimaX −0.02 ± 0.02 ppm) (Figure 2D). This confirms that spectrum calibration, based on hundreds of pet food-specific masses, was successfully executed for both systems. The average absolute mass error (solariX 0.24 ± 0.08 ppm; scimaX 0.20 ± 0.02 ppm) demonstrates slight advantages of the new cell generation, particularly evident in sample 3 (Figure 2E). Given the high number of features and immense dynamic range in the spectra (intensity range of 5 × 10^6 to 2 × 10^{10}), it is likely that space-charge effects[21,23] caused by adduct signals significantly influenced the results. While a specific density calibration[22] eliminated systematic local mass errors,[30] a global negative impact on mass accuracy in an overloaded cell persisted (Figure S1). Here, the benefits of the higher sensitivity of the dynamically harmonized cell and the associated 4-fold dilution of samples in the scimaX system become apparent. The m/z distribution, when considering matched ion transfer parameters, further highlights the improved sensitivity of the ParaCell in the lower mass range (average m/z solariX 367.5 ± 22.6; scimaX m/z 340.4 ± 22.7) (Figure 2F).

https://doi.org/10.1021/acs.analchem.5c00488
Anal. Chem. 2025, 97, 8491−8498

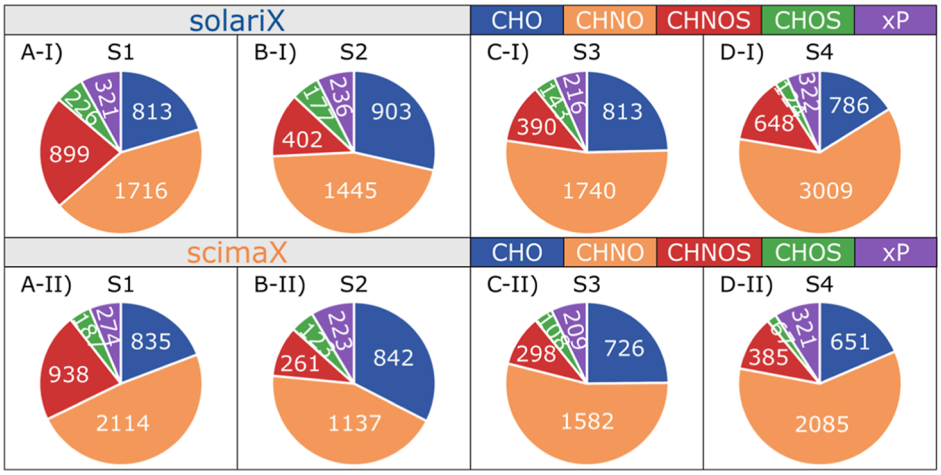

Figure 3. Chemical space distribution of the different pet food samples (A–D) measured on the solariX (I) and scimaX (II) setups. The chemical spaces are color-coded: clockwise CHO (blue), CHNO (orange), CHNOS (red), CHOS (green), and xP (purple). Chloride adducts are converted into the respective $[M - H]^-$ ions in silico. All compositions featuring at least one phosphate atom are considered (CHNOS)P or xP.

Both systems demonstrated stable, sample-independent performance across most quality parameters, operating at a comparable and interoperable level with slightly better detection of lower mass signals in the ParaCell. The scimaX ParaCell's higher sensitivity, allowing for greater sample dilution, reduced susceptibility to space-charge effects,[21,23] leading to more stable mass errors. Moreover, the advancements in both technology and sensitivity have significantly reduced the required scan count and accumulation time, leading to shorter measurement durations on the scimaX system, thereby greatly increasing throughput (Figure 1; 4.4 versus 10.4 min).

Comparison of the Captured Molecular Profiles. The similar values of instrumental performance parameters indicate technical comparability between the 12 T solariX infinity cell and the 7 T scimaX ParaCell setups. However, whether both setups provide the same molecular information requires a separate evaluation. Depending on the sample and setup, the proportion of signals detected by both instruments in their respective spectra (at least two out of three replicates) ranges from 55% to 78% (Figure S2). The numbers increase to 90%–95% when only the compositions within the 25th percentile of the highest intensity are considered. This is expectedly higher than the values found by Hawkes et al.[14] in their ring trial, which compared multiple laboratories and instruments. Such overlapping ratios are a satisfactory outcome, considering the intrinsically complex and challenging matrix and the nearly 20 year generational difference between the setups. Alongside the general overlap of mass signals, the chemical spaces of the samples are captured almost identically in both systems (Figure 3). Between the instrument setups, the absolute root mean square deviation value across all chemical spaces, which is significantly influenced by large chemical spaces (CHO, CHNO), is ±2.16% of the overall distribution. Relative fluctuations in compositional spaces are ±16.78%, particularly influenced by less abundant chemical spaces (CHOS, xP).

While the mere detection and presence of formulas remain independent of intensity values, multivariate statistical methods rely on abundance comparisons. As shown in Figure 1, the data structures, particularly noise levels and intensity ranges, differ significantly between the two systems. A PCA comparison of measurements normalized across the entire merged data matrix is predictably uninformative, as the higher intensity values of the solariX system overshadow any differentiation in the scimaX measurements (Figure S3). A common approach to comparing such spectra is to reference intensity values to their proportion of the total ion load, thus representing relative abundances.[14,19] However, due to the overwhelming influence of adduct ions on the total charge in many life sciences samples,[17,31−36] including pet food, this approach is arguably not as effective as for NOM/DOM samples with lower concentration or rather intensity dynamic ranges. To achieve comparability of the data from two setups, the intensity values of the mass signals were z-score-normalized across samples within each instrumental setup. This approach yields relative intensity values for each feature across all measurements within a given system. Alternative normalization methods, such as TIC normalization and interinstrument normalization, were also evaluated but did not provide adequate comparability (data not shown). Although the z-score normalization method is independent of the inherently large dynamic ranges of major adduct signals, it cannot fully eliminate the impact of the suppression effects. The median coefficient of variation (CV) of replicate measurements within the systems ranged from 13.5% to 42.7% (solariX) and from 13.4% to 23.8% (scimaX). The median CV for the normalized intensity values of features detected across all replicates in both systems ranged from 23.4% (sample 1) to 49.2% (sample 3). When considering only the compositions within the top 25th percentile of highest abundance, these values decrease to 15.5%–29.5%. The variability between the two systems, therefore, is moderately higher than within each system and is in a similar range as the variability observed in FT-ICR-MS spectra of the same sample over multiple years (CV of 39 ± 14% [13]). In general, sources of measurement variability can be primarily attributed to the direct infusion method, which is inherently susceptible to fluctuations in ionization dynamics. This effect is particularly pronounced in complex samples, where adduct formation can lead to saturation of the ICR cell and space-charge effects.[21] These sample-intrinsic phenomena are difficult to predict and were observed to a greater extent in the solariX system, especially in Sample 3. Beyond ionization effects, structural differences between instruments, such as variations in the ion path and ICR cell design, are also critical

https://doi.org/10.1021/acs.analchem.5c00488
Anal. Chem. 2025, 97, 8491−8498

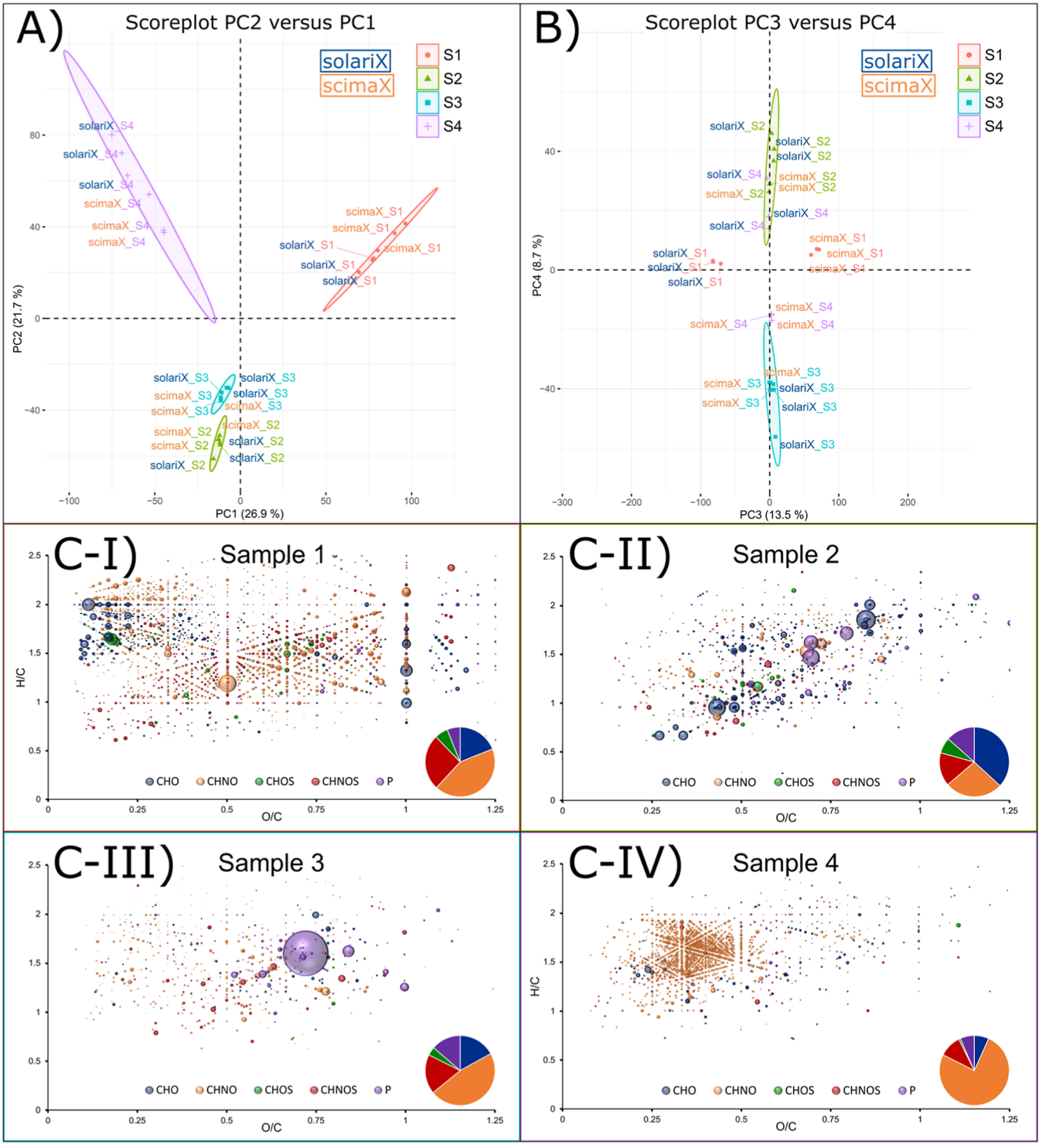

Figure 4. PCA analysis of the within-system normalized data set (A,B) and the characteristic molecular profiles of the pet food samples in the van Krevelen representation (C). In the first and second principal component, sample 1 and sample 4 are distinguished based on their chemical signature (A). The third and fourth PC indicate a differentiation of the solariX and scimaX measurements of sample 1 and achieve a clear separation of sample 2 and 3, respectively. Confidence intervals (95%) are indicated as ellipses. The underlying loadings plot is shown in Figure S4.

contributors to variability. Key factors in sample introduction and ionization were accounted for using identical ion sources and autosampler units. Due to the strictly controlled study design and the transport of identical sample aliquots under frozen conditions, the contribution of sample preparation to intersystem variability is expected to be minimal.

To assess the impact of intensity variations on the comparability of holistically detected molecular profiles between the systems, multivariate PCA was performed (Figure 4). In the first principal component (26.9%), sample 1 (wet chicken variety) of both systems forms a distinct cluster, separating them from other samples (Figure 4A). The second principal component (21.7%) differentiates the molecular

https://doi.org/10.1021/acs.analchem.5c00488
Anal. Chem. 2025, 97, 8491−8498

profiles of sample 4 (dry chicken variety) from those of sample 2 (dry cheese variety) and sample 3 (dry tuna variety). Despite the proximity of sample 2 and 3 in the score plot, indicating a high degree of molecular similarity, the clusters are clearly separated within the 95% confidence intervals. The molecular essence of all samples was consistent between measurements on the solariX and scimaX systems, with ANOVA revealing highly significant differences among sample groups ($p < 2 \times 10^{-16}$). Further differentiation of Samples 2 and 3 is achieved in PC4 (8.7%) (Figure 4B). The molecular profiles characteristic of the sample signatures (Figure 4C), which were concordant between the solariX and scimaX setups, were extracted based on feature density in the corresponding loading plot (Figure S4). Residual differences between the systems were evident in the separation of solariX and scimaX measurements for Sample 1 and Sample 4 along principal components four and three, respectively (Figures S4D and S6). However, a systematic difference between the instrumental setups was not observed, as indicated by a very low Cohen's d of 0.02.

In conclusion, the comparison of complex pet food samples on two thoroughly aligned FT-ICR-MS setups—instruments from different generations (12 T solariX vs. Seven T scimaX) and cell types (Infinity Cell vs. ParaCell)—revealed similar and interoperable instrument performance in terms of signal-to-noise ratios, resolution, and mass errors. Despite the lower magnetic field strength, the scimaX/ParaCell's enhanced sensitivity was evident, resulting in a higher dilution factor and therefore reduced susceptibility to cell overloading effects such as space-charge. Naturally, direct infusion or flow injection mass spectrometry is sensitive to sample preparation and introduction parameters, such as the autosampler and ESI source. In our setup these are identical and meticulously aligned, but the effects of necessary dilution adjustments still affect the ionization environment in ESI and therefore mass signal abundance.[37] Consequently, the overlap of individual mass signals could not surpass a notably substantial value of 78% (average 66%). For higher-intensity signals, the value increases to 95% (average of 92%), indicating that the deep fingerprint is more affected than the abundant features. The various compositional spaces (CHNOSP) of the samples are detected in remarkably consistent representation across both systems (±2.16%). Appropriate data processing can harmonize molecular profiles from different generations of systems and ICR cells. In multivariate analyses (PCA), the characteristic signatures of individual samples dominate the principal components without systematic bias from the systems. Especially with challenging and heterogeneous sample types, such as pet food, the strong interoperability of systems from different generations and cell types still exhibits some degree of sample dependency.

CONCLUSIONS

Our study demonstrates that with careful adjustment of the instrument setups, the comparability of molecular profiles can be achieved, ensuring that extensive databases generated by previous-generation instruments remain relevant and useful in long-term projects. Stable instrument quality parameters such as mass accuracy, resolving power, and signal-to-noise ratios form the basis for comparable detection of the molecular essence of the samples, in terms of both chemical spaces and the observed compositional mass signals. The unmatched mass accuracy and resolution of FT-ICR-MS enable excellent alignment of spectra in direct-infusion mode, based on the precisely determined masses of ions. The remaining differences between the instruments are nonsystematic and sample-specific and can be attributed to the individually optimized methods. Even though we placed great emphasis on harmonization, adjustments to the methodology are necessary to accommodate advanced technology and achieve a realistic comparison scenario. We demonstrate that compositional data in direct-infusion methods, when sufficient resolution is provided and harmonization is achieved, maintain their enduring value for extended projects, follow-up studies, or extensive databases. An upgrade of instrument systems, aimed at achieving faster acquisition rates, higher throughput, sensitivity, or more sustainable operational costs, can be implemented, while preserving the integrity and value of the existing data. Undoubtedly, advanced techniques, made possible by significantly accelerated acquisition rates, such as spectral stitching, chromatography, or ion mobility hyphenation, will find broader application in the future and provide new data structures, whose interoperability and harmonization must be similarly evaluated.

ASSOCIATED CONTENT

Data Availability Statement

The data sets generated and/or analyzed during the study are made available from the corresponding authors on reasonable request.

Supporting Information

The Supporting Information is available free of charge at https://pubs.acs.org/doi/10.1021/acs.analchem.5c00488.

FT-ICR-MS instrument and measurement parameters, overview of the mass spectra and their annotation error distribution, Venn diagram of the common signals between the solariX and scimaX, PCA score plot of the solariX and scimaX analyses based, PCA score plots and loadings plots of the solariX and scimaX, van Krevelen diagrams of the mass signals of the samples in both systems, and van Krevelen diagrams of the mass signals characteristic for specific samples (PDF)

AUTHOR INFORMATION

Corresponding Authors

Philippe Schmitt-Kopplin − *Analytical Food Chemistry, TUM School of Life Sciences, Technical University of Munich, 85354 Freising, Germany; Analytical BioGeoChemistry, Helmholtz Association, 85764 Neuherberg, Germany*; Email: schmitt-kopplin@tum.de

James W. Marshall − *Waltham Petcare Science Institute, Mars Petcare, Waltham on the Wolds, LE14 4RT Melton Mowbray, U.K.*; orcid.org/0000-0003-3352-7629; Email: james.marshall@effem.com

Authors

Stefan A. Pieczonka − *Analytical Food Chemistry, TUM School of Life Sciences, Technical University of Munich, 85354 Freising, Germany; Analytical BioGeoChemistry, Helmholtz Association, 85764 Neuherberg, Germany*; orcid.org/0000-0003-0939-9858

Mary J. Thomas − *Waltham Petcare Science Institute, Mars Petcare, Waltham on the Wolds, LE14 4RT Melton Mowbray, U.K.*

Complete contact information is available at:

https://doi.org/10.1021/acs.analchem.5c00488
Anal. Chem. 2025, 97, 8491−8498

https://pubs.acs.org/10.1021/acs.analchem.5c00488

Author Contributions

All authors contributed to the study's conception, design, and administration. SAP and MJT prepared the sample. SAP and MJT designed the data analysis methodology. SAP and MJT performed the measurements. SP performed data processing, statistical analysis, and visualization. PSK and JWM provided the infrastructure for sample preparation, measurements, and data processing. SAP and MJT wrote the first draft of the manuscript. All authors contributed to manuscript revision, read, and approved the submitted version.

Notes

The authors declare the following competing financial interest(s): This research was funded by Mars Petcare UK. MJT and JWM were employed by Mars Petcare UK (Waltham Petcare Science Institute, Waltham on the Wolds, UK), a subsidiary of Mars Inc. that focuses on fundamental science research to support the Mars Petcare business.

Declaration of Generative AI and AI-assisted technologies in the writing process: During the preparation of this work author SAP used DeepL (DeepL SE; October 2024) and ChatGPT4.0 (OpenAI Inc.) to improve readability and language of sentences in a draft version of the manuscript. All authors reviewed and edited the content to ensure clarity of message and scientific accuracy and take full responsibility for the content of the publication.

REFERENCES

(1) Schmitt-Kopplin, P.; Kanawati, B. *Fundamentals and Application of Fourier Transform Mass Spectrometry*; Elsevier, 2019.

(2) Nikolaev, E. N.; Boldin, I. A.; Jertz, R.; Baykut, G. *J. Am. Soc. Mass Spectrom.* **2011**, *22* (7), 1125−1133.

(3) Lioznov, A.; Nikolaev, E. *Eur. J. Mass Spectrom.* **2023**, *29* (2), 97−101.

(4) Tiquet, M.; La Rocca, R.; Kirnbauer, S.; Zoratto, S.; Van Kruining, D.; Quinton, L.; Eppe, G.; Martinez-Martinez, P.; Marchetti-Deschmann, M.; De Pauw, E.; et al. *Anal. Chem.* **2022**, *94* (26), 9316−9326.

(5) Xu, J.; Li, M.; Marzullo, B.; Wootton, C. A.; Barrow, M. P.; O'Connor, P. B. *J. Am. Soc. Mass Spectrom.* **2022**, *33* (8), 1499−1509.

(6) Cho, E.; Witt, M.; Hur, M.; Jung, M. J.; Kim, S. *Anal. Chem.* **2017**, *89* (22), 12101−12107.

(7) Thomas, M. J.; Collinge, E.; Witt, M.; Palacio Lozano, D. C.; Vane, C. H.; Moss-Hayes, V.; Barrow, M. P. *Sci. Total Environ.* **2019**, *662*, 852−862.

(8) Palacio Lozano, D. C.; Gavard, R.; Arenas-Diaz, J. P.; Thomas, M. J.; Stranz, D. D.; Mejia-Ospino, E.; Guzman, A.; Spencer, S. E. F.; Rossell, D.; Barrow, M. P. *Chem. Sci.* **2019**, *10* (29), 6966−6978.

(9) Kew, W.; Myers-Pigg, A.; Chang, C.; Colby, S.; Eder, J.; Tfaily, M.; Hawkes, J.; Chu, R.; Stegen, J. *EGUsphere* **2022**, 1−26.

(10) Thomas, M. J.; Chan, H. Y. H.; Palacio Lozano, D. C.; Barrow, M. P. *Anal. Chem.* **2022**, *94* (12), 4954−4960.

(11) Ruddy, B. M.; Hendrickson, C. L.; Rodgers, R. P.; Marshall, A. G. *Energy Fuels* **2018**, *32* (3), 2901−2907.

(12) Patriarca, C.; Hawkes, J. A. *J. Am. Soc. Mass Spectrom.* **2021**, *32* (1), 394−397.

(13) Woodward, S. E.; Pieczonka, S. A.; Hertzog, J.; Haydock, R.; Thomas, M. J.; Roullier-Gall, C.; O'Flynn, C.; Uhl, J.; Rychlik, M.; Schmitt-Kopplin, P.; et al. *Talanta* **2025**, *286*, 127514.

(14) Hawkes, J. A.; D'Andrilli, J.; Agar, J. N.; Barrow, M. P.; Berg, S. M.; Catalán, N.; Chen, H.; Chu, R. K.; Cole, R. B.; Dittmar, T.; et al. *Limnol. Oceanogr.:Methods* **2020**, *18* (6), 235−258.

(15) Zherebker, A.; Kim, S.; Schmitt-Kopplin, P.; Spencer, R. G. M.; Lechtenfeld, O.; Podgorski, D. C.; Hertkorn, N.; Harir, M.; Nurfajin, N.; Koch, B.; et al. *Pure Appl. Chem.* **2020**, *92* (9), 1447−1467.

(16) Kirwan, J. A.; Broadhurst, D. I.; Davidson, R. L.; Viant, M. R. *Anal. Bioanal. Chem.* **2013**, *405* (15), 5147−5157.

(17) Forcisi, S.; Moritz, F.; Thompson, C. J.; Kanawati, B.; Uhl, J.; Afonso, C.; Bader, C. D.; Barsch, A.; Boughton, B. A.; Chu, R. K.; et al. *J. Am. Soc. Mass Spectrom.* **2022**, *33* (12), 2203−2214.

(18) Kido Soule, M. C.; Longnecker, K.; Giovannoni, S. J.; Kujawinski, E. B. *Org. Geochem.* **2010**, *41* (8), 725−733.

(19) Clark, T. N.; Houriet, J.; Vidar, W. S.; Kellogg, J. J.; Todd, D. A.; Cech, N. B.; Linington, R. G. *J. Nat. Prod.* **2021**, *84* (3), 824−835.

(20) Kirwan, J. A.; Weber, R. J.; Broadhurst, D. I.; Viant, M. R. *Sci. Data* **2014**, *1*, 140012.

(21) Jeffries, J. b.; Barlow, S. E.; Dunn, G. H. *Int. J. Mass Spectrom.* **1983**, *54*, 169−187.

(22) Smirnov, K. S.; Forcisi, S.; Moritz, F.; Lucio, M.; Schmitt-Kopplin, P. *Anal. Chem.* **2019**, *91*, 3350−3358.

(23) Francl, T. J.; Sherman, M. G.; Hunter, R. L.; Locke, M. J.; Bowers, W. D.; McIver, R. T. *Int. J. Mass Spectrom.* **1983**, *54*, 189−199.

(24) Kanawati, B.; Bader, T. M.; Wanczek, K. P.; Li, Y.; Schmitt-Kopplin, P. *Rapid Commun. Mass Spectrom.* **2017**, *31* (19), 1607−1615.

(25) Tziotis, D.; Hertkorn, N.; Schmitt-Kopplin, P. *Eur. J. Mass Spectrom.* **2011**, *17*, 415−421.

(26) Pieczonka, S. A.; Hemmler, D.; Moritz, F.; Lucio, M.; Zarnkow, M.; Jacob, F.; Rychlik, M.; Schmitt-Kopplin, P. *Food Chem.* **2021**, *361*, 130112.

(27) Hertkorn, N.; Frommberger, M.; Witt, M.; Koch, B. P.; Schmitt-Kopplin, P.; Perdue, E. M. *Anal. Chem.* **2008**, *80*, 8908−8919.

(28) Schmitt-Kopplin, P.; Hemmler, D.; Moritz, F.; Gougeon, R. D.; Lucio, M.; Meringer, M.; Muller, C.; Harir, M.; Hertkorn, N. *Faraday Discuss.* **2019**, *218* (0), 9−28.

(29) Pieczonka, S. A.; Paravicini, S.; Rychlik, M.; Schmitt-Kopplin, P. *Front. Chem.* **2021**, *9*, 715372.

(30) Masselon, C.; Tolmachev, A. V.; Anderson, G. A.; Harkewicz, R.; Smith, R. D. *J. Am. Soc. Mass Spectrom.* **2002**, *13*, 99−106.

(31) Pieczonka, S. A.; Dzemajili, A.; Heinzmann, S. S.; Rychlik, M.; Schmitt-Kopplin, P. *Food Chem.* **2025**, *463* (Pt 4), 141432.

(32) Pieczonka, S. A.; Zarnkow, M.; Ampenberger, F.; Gastl, M.; Rychlik, M.; Schmitt-Kopplin, P. *Front Nutr* **2023**, *10*, 1243503.

(33) Marshall, J. W.; Schmitt-Kopplin, P.; Schuetz, N.; Moritz, F.; Roullier-Gall, C.; Uhl, J.; Colyer, A.; Jones, L. L.; Rychlik, M.; Taylor, A. J. *Food Chem.* **2018**, *242*, 316−322.

(34) Zhang, J.; McCombie, G.; Guenat, C.; Knochenmuss, R. *Drug Discovery Today* **2005**, *10* (9), 635−642.

(35) Han, J.; Danell, R. M.; Patel, J. R.; Gumerov, D. R.; Scarlett, C. O.; Speir, J. P.; Parker, C. E.; Rusyn, I.; Zeisel, S.; Borchers, C. H. *Metabolomics* **2008**, *4* (2), 128−140.

(36) Islam, S.; Alam, M. B.; Ahmed, A.; Lee, S.; Lee, S. H.; Kim, S. *Food Chem.* **2020**, *332*, 127377.

(37) Zhou, S.; Hamburger, M. *Rapid Commun. Mass Spectrom.* **1995**, *9* (15), 1516−1521.

https://doi.org/10.1021/acs.analchem.5c00488
Anal. Chem. 2025, 97, 8491−8498